

Study of the Interference in Target Seed Germination Caused by Dienamides and Epoxy Derivatives, in the Search for New Herbicides

Danielle S. Ramos,^{1b} Elson S. Alvarenga,^{1b}*,^a Júnio G. Silva,^{1b}*,^a Cristiane I. Cerceau,^{1b}*,^a Suélen K. Sartori,^{1b}*,^a Vania M. T. Carneiro,^{1b}*,^a and Denilson F. Oliveira^{1b}*,^b

^aDepartamento de Química, Universidade Federal de Viçosa (UFV), Av. Peter Henry Rolfs, s/n, Campus Universitário, 36570-900 Viçosa-MG, Brazil

^bDepartamento de Química, Universidade Federal de Lavras, 37200-900 Lavras-MG, Brazil

The indiscriminate use of herbicides makes weeds resistant, increasing the demand for more efficient herbicides. Novel potential herbicides were prepared from sorbic acid, being 8 dienamides and 6 epoxides. Subsequently, phytotoxic activities of sorbic acid and 14 synthesized compounds were evaluated against sorghum, onion, cucumber, lettuce, and beggartick seeds. Furthermore, the protein target of the most active substance in plants was identified *in silico*. Among the tested compounds, (2*E*,4*E*)-*N*-(*p*-fluorophenyl)hexa-2,4-dienamide (**2c**), (2*E*,4*E*)-*N*-(*o*-naphthyl)hexa-2,4-dienamide (**2d**), (*E*)-*N*-methylphenyl-3-((2*R*,3*R*)-3-methyloxiran-2-yl)acrylamide (**3b**), (*E*)-*N*-bromophenyl-3-((2*R*,3*R*)-3-methyloxiran-2-yl)acrylamide (**3e**), and (*E*)-*N*-methoxyphenyl-3-((2*R*,3*R*)-3-methyloxiran-2-yl)acrylamide (**3f**) showed pronounced inhibitory activities, both of shoots and roots, making them candidates for promising herbicides. All compounds altered seed development, and compounds **2c**, **2d**, **3b**, **3e**, and **3f** presented equal or superior results to the commercial control herbicide *S*-metolachlor. Docking studies suggest that enzyme mitogen-activated protein kinase can be the target of those compounds.

Keywords: sorghum, onion, cucumber, beggartick, docking

Introduction

According to the United Nations,^{1,2} the population will grow by the year 2050 to something around 9.7 billion people worldwide. This rapid and continuous population expansion is the main factor in consumption growth, which should boost food production by 70%.³ Meeting this demand is currently impossible without the use of agrochemicals that aim to ensure higher crop yields by combating pests and adverse conditions.^{4,5}

Weed species daily infest fields and reduce crop yields through competition for resources such as water, light, and nutrients.⁶ In China, weeds occupy 35.8 million hectares out of 114.36 million hectares of cultivated land in the country, resulting in losses equivalent to 16.5 million tons of grain.⁷ In sub-Saharan Africa, rice crops suffer annual losses of up to 2.2 million tons of their agricultural production for the same reason.⁸ In Brazil, just in the soybean crop, weeds cause losses of approximately 2 billion dollars *per year*.⁹

Therefore, studies are needed to develop control methods that are effective and selective in combating weeds to ensure greater productivity in the agro-industrial sector.

Faced with various strategies that make agriculture more productive and profitable, biological, genetic and cultivation techniques can be used,¹⁰ but the use of chemical control has been the main method of weed management because it is more efficient and economical.^{11,12} Although chemical herbicides are the main control tool, their repeated and inappropriate use, coupled with other factors, has resulted in mutations, and the selection of resistant weeds.¹³ Therefore, researchers seek to develop new products to obtain a better spectrum of action and effectiveness in weed control.¹⁴

Among the variety of compounds that exhibit herbicidal activity, the dienamide subclass is promising.¹⁵ Usually, dienamides are found in several natural compounds, which are responsible for a variety of activities. For example, trichostatin A (**I**) has antifungal and anticancer activity; pellitorine (**II**) has insecticidal and cytotoxic activity; and piperlonguminine (**III**) has antibacterial, antifungal, antitumor, anticoagulant, and anti-inflammatory activities (Figure 1).¹⁶

*e-mail: elson@ufv.br

Editor handled this article: Andrea R. Chaves (Associate)



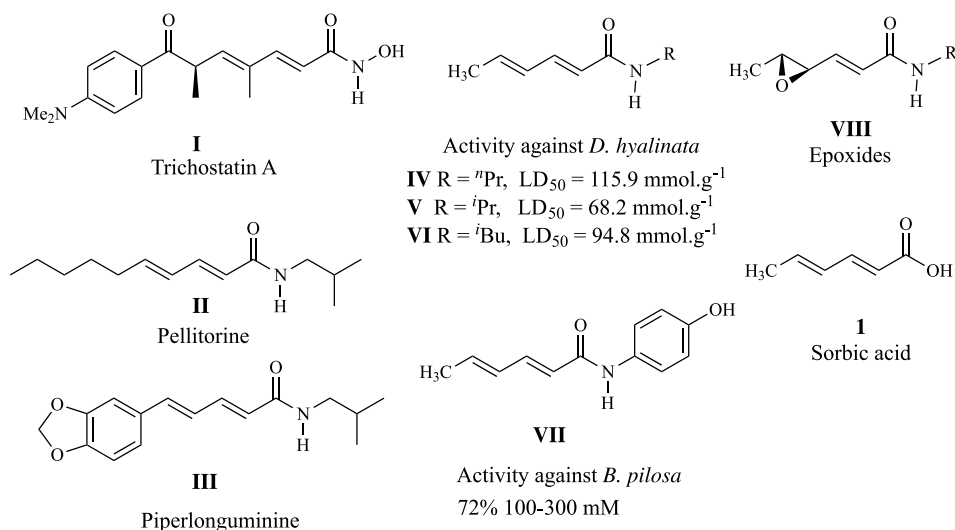


Figure 1. Bioactive sorbic acid, dienamides, and epoxides reported in the literature, LD₅₀: lethal doses to cause 50% mortality.

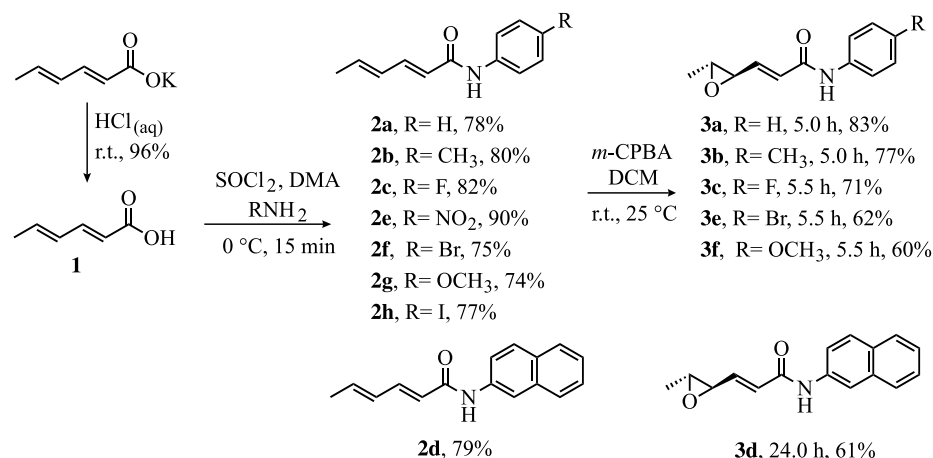
In the last years, our research group carried out studies to obtain dienamides with potential biological activity.¹⁷⁻¹⁹ For example, the dienamides **IV-VII** (Figure 1) had better results than the commercial insecticide bifenthrin against *Diaphania hyalinata*.^{17,18} In a more recent study conducted in our group,¹⁹ a series of dienamides were synthesized and evaluated for their pre-emergent herbicidal activities against onion and cucumber, in which the compound **VII** (Figure 1) showed the best herbicidal potential.

Using an easy-to-apply methodology that does not require chromatographic purification of the product, this work presents the syntheses of *N*-aryldienamides from an inexpensive and low-toxic compound as a starting material, the sorbic acid (**1**). Additionally, highly regioselective mono-epoxidation of dienamides produced epoxides (**VIII**) (Figure 1).²⁰ All synthesized compounds were evaluated for their herbicidal activities against mono and dicotyledonous plants (Scheme 1). Finally, docking studies were performed for two of the most active compounds.

Experimental

Chemicals and general experimental procedures

All reactions were analyzed by thin layer chromatography (TLC) and observed in an ultraviolet (UV) chamber under a 254 nm lamp.²¹ Melting point temperatures were evaluated on an MQAPF-302 (Microchemistry, Brazil) apparatus and were uncorrected. Infrared (IR) spectra were acquired using a Varian 660-IR FT-IR spectrophotometer (equipped with GLADI-ATR) using the attenuated total reflectance (ATR) method. Nuclear magnetic resonance (NMR) spectra were recorded on a Bruker Advance DRX 400 MHz spectrometer using CDCl₃ and deuterated dimethyl sulfoxide (DMSO-*d*₆) as solvents. ¹H NMR chemical shifts were reported using the residual signal of CHCl₃ (δ 7.27) and DMSO-*d*₅ (δ 2.50) as references. ¹³C NMR chemical shifts were recorded using the CDCl₃ signal (δ 77.0) and the DMSO-*d*₆ signal (δ 39.5) as a reference. Mass spectra were obtained on a Shimadzu



Scheme 1. Syntheses and yields of the dienamides **2a-2h** and epoxy amides **3a-3f** from potassium sorbate.

GC-MS-QP5050A (Kyoto, Japan) mass spectrometer. The instrument was operated at 70 eV, and the scanning range was set between 29-400 Da. The chromatographic conditions consisted of a fused silica capillary column (30 m × 0.22 mm) with a DB5 stationary phase (0.25 μm film thickness). Helium was used as the carrier gas, with a flow rate of 1.8 mL min⁻¹. The temperature was programmed to remain at 60 °C for 2 min, followed by an increase of 3 °C min⁻¹ until it reached 240 °C, which was maintained for 15 min. The injector temperature was set to 220 °C, while the detector (or interface) temperature was set to 240 °C. An injection volume of 1.0 μL (1 mg of compound in 1 mL of dichloromethane) was used, with a partition ratio of the injected volume of 1:10 and a column pressure of 166 kPa. The ¹H and ¹³C NMR spectra of the dienamides and epoxides can be found in the Supplementary Information (SI) section.

Synthetic procedures

General procedure for the preparation of sorbic acid **1**

Into a round-bottomed flask were poured potassium sorbate (20.0 g, 1 mmol) and 1.0 mol L⁻¹ hydrochloric acid solution (200.0 mL), and the reaction mixture was stirred for 5 min at room temperature. After this time, the reaction mixture was transferred to a separating funnel and extracted with three portions of dichloromethane (DCM, 200.0 mL). The organic phases were combined, dried over anhydrous sodium sulfate, and filtered. The solvent was removed under reduced pressure to afford sorbic acid **1** (14.3 g, 96% yield).

General procedure for the preparation of the dienamides **2a-2h**

Thionyl chloride (0.3 mL, 4.1 mmol) was added to an ice bath cooled solution of sorbic acid **1** (0.500 g, 4.46 mmol) dissolved in *N,N*-dimethylacetamide (DMA) (3.0 mL) in a two neck round bottomed flask. The mixture was stirred at 0 °C under nitrogen atmosphere for 1 h. The aniline (4.5 mmol) was added to the reaction mixture under magnetic stirring for 15 min at 20 °C. Iced distilled water (30.0 mL) was added to the reaction mixture and the precipitate was collected by filtration under vacuum and placed in the desiccator for 5 days.²² Yields for compounds **2a-2h** ranged from 74 to 90% (Scheme 1).

General procedure for the preparation of epoxy amides **3a-3f**

The amide **2a-2g** (0.8 mmol) was dissolved in anhydrous DCM (5.0 mL) and then *m*-chloroperbenzoic acid (MCPBA) (1.6 mmol) was added. The reaction mixture was stirred at room temperature and the reaction was followed by gas chromatography coupled with mass

spectrometer (GC-MS). The excess MCPBA was consumed by reaction with aqueous sodium sulfite (Na₂SO₃) solution (30.0 mL, 4.8 mmol) and the reaction mixture was transferred to a separating funnel. The aqueous phase was extracted with three fractions of DCM (3 × 20.0 mL). The combined organic phases were washed with potassium carbonate solution (30 mL, 6.4 mmol) and the aqueous phase was extracted with three portions of DCM (3 × 20.0 mL). The organic phases were collected and dried over anhydrous sodium sulfate. The mixture was filtered and concentrated under reduced pressure.²⁰ The residue was purified by silica gel column chromatography using a mixture of hexane and ethyl acetate (2:1 v/v), to afford the epoxides **3a-3f** in moderate yields (59-83%). The structures of the epoxides, yield, and reaction time are summarized in Scheme 1.

Herbicidal bioassays-general procedures

Pre-emergent activities of all compounds (**1**, **2a-2h**, and **3a-3f**) were evaluated against onion (*Allium cepa* L. “*Baia Periforme*”), sorghum (*Sorghum bicolor* L.), lettuce (*Lactuca sativa* L. “*Butter*”), cucumber (*Cucumis sativus* L. “*Caipira*”), and beggartick seeds (*Bidens pilosa* L.). Except for beggartick seeds that were collected in July 2019 in the Córrego São João, located in Viçosa, Minas Gerais, Brazil (altitude: 889 m, latitude: 20°42'22" South and longitude: 42°54'08" West, coordinates), the others were obtained commercially. The dormancy break of beggartick seeds was done by soaking them in distilled water (20 °C) for 24 h.²³

The substances to be evaluated were dissolved in 0.3 mL dimethylsulfoxide (DMSO) and the volume was completed with previously boiled and cooled distilled water to 100 mL in a volumetric flask, to obtain the solutions in the concentrations of 500, 250, 100, and 50 μmol L⁻¹.

A total of 20 seeds of each plant were used in the bioassays. The experiment was performed in triplicate and the plates were properly identified, sealed with plastic film, and taken to a germination chamber (biological oxygen demand (BOD)) at 25 °C, in the absence of light, for 120 h (5 days). After this time, the germinated seeds were frozen at 0 °C for 24 h to stop the growth and to facilitate the measurement step. The seeds were removed from the freezer, lined up on black paper, and photographed. The analyses of the images were done digitally in the program ImageJ.²⁴

The negative control used was an aqueous 0.3% DMSO solution (v/v) and the positive control was an aqueous solution of the commercial *S*-metolachlor herbicide, using the same concentrations of synthesized compounds.

Data are presented by bar graphs with percentage inhibition/stimulation of seed and root parts in relation to controls. Thus, zero represents the control, positive values

represent stimulus and negative values represent inhibition of the studied parameters. In addition to the percentages, bars with standard deviations on the stimulus and inhibition are also presented.

Computational study-pharmacophoric search

ACD ChemSketch 12.01 (Advanced Chemical Development 2012),²⁵ OpenBabel 3.0.0,²⁶ Open3Dalign 2.3,²⁷ and MOPAC 2016²⁸ were used to obtain the most stable conformations of compounds **2c** and **2d**, which underwent a pharmacophoric search using Lisica 1.0.1²⁹ and the Ligand Expo database.³⁰ All proteins whose ligands had Tanimoto scores ≥ 0.5 in the pharmacophoric search and were not chemically bound to the proteins were selected for the next step.

MSMS computes solvent excluded surfaces on a protein structure. Generally, MSMS is used to calculate residue depths relative to the protein surface using a PDB file as an input.³¹

Amino acid sequences in plant genomes

The amino acid sequences of selected proteins (pharmacophoric search) were used to search for similar proteins in the genomes of *Allium* spp. (taxid:4678), *Bidens* spp. (taxid:42336), *Cucumis* spp. (taxid:3655), *Lactuca* spp. (taxid:4235), *Sorghum* spp. (taxid:4557), and of plants in general (taxid:3193), through the database of the National Center for Biotechnology Information,³² using the Blastp 2.11.0+ software³³ with DELTA-BLAST (Domain Enhanced Lookup Time Accelerated BLAST)³⁴ set to default values. Only those proteins with scores above 200 for searches carried out in the genomes of *Cucumis* spp., *Lactuca* spp., and *Sorghum* spp. were further selected.

Protein tyrosine phosphatase

The three-dimensional structures of the protein tyrosine phosphatase 1c84,³⁵ and all proteins with similarities of amino acid sequences equal to 100% in relation to the amino acid sequence of 1c84, were obtained from the RCSB Protein Data Bank.³⁶ The amino acids sequences were aligned in the program Ugene 37.0,³⁷ through 10 iterations with Clustal Omega 1.2.4.³⁸ Then, Hamming dissimilarity was calculated by Ugene, considering the gaps. The three-dimensional structures underwent removal of alternation locations with VMD 1.9.3³⁸ and alignment with Lovoalign 21.027.³⁹ The three-dimension structures of cyclophilins produced by *Arabidopsis thaliana* (L.) Heynh. and *Avena sativa* L., with amino acid sequence similarities

equal to or higher than 30% in relation to 1c84, were also obtained from the RCSB Protein Data Bank and submitted to the same procedure. Only those proteins (produced by plants or not) that were not mutants and had no missing residue in the binding site or close to it, were selected for the next step.

Using LS-align J201704171741⁴⁰ for rigid alignment, the most stable conformations of compounds **2c** and **2d** underwent superposition to the three-dimensional structures of the compounds OLN (3-[(carboxylatocarbonyl)amino]naphthalene-2-carboxylate), OAI (6-[(carboxylatocarbonyl)amino]-1*H*-indole-5-carboxylate), OBA (2-[(carboxylatocarbonyl)amino]benzoate), OPA (2-[(carboxylatocarbonyl)amino]-4,7-dihydro-5*H*-thieno[2,3-*c*]pyran-3-carboxylate), OTA (2-[(carboxylatocarbonyl)amino]-4,5,6,7-tetrahydrothieno[2,3-*c*]pyridin-6-ium-3-carboxylate), and OLI (2-[(carboxylatocarbonyl)amino]-5-iodobenzoate), whose protonation states at pH 7 were determined by calculating the pK_a values using the Marvin Sketch 19.21.⁴¹ These substances were used with the same conformations and positions observed in the complexes formed with the protein tyrosine phosphatases 1c84,⁴² 1c83,⁴² 1c85,⁴² 1c87,⁴³ 1c88,⁴³ and 1ecv,⁴² respectively. Then, the coordinates of **2c**, **2d**, OLN, OAI, OBA, OPA, OTA, and OLI, were manually combined with the coordinates of the protein tyrosine phosphatases 1c84, 1c83, 1c85, 1c87, 1c88, and 1ecv. Using Chimera 1.15⁴⁴ the resulting complexes underwent hydrogen addition considering steric factors and the formation of hydrogen bonds. Charges were added to the proteins according to the AMBER ff14SB force field,⁴⁵ while the AM1-BCC method⁴⁶ was applied to calculate charges for the other compounds using the Antechamber⁴⁷ module of the program Chimera. The complexes were then submitted to energy minimization in the same program through 300 steepest descent steps of 0.02 Å, followed by 30 conjugate gradient steps. The update interval during the minimization was equal to 10.

For each of the complexes, the enzyme structure and the ligand were converted to the pdbqt format using AutodockTools 1.5.7rc1.⁴⁸ Then, affinities of the ligands for the enzymes were calculated by QuickVina 2.1^{49,50} and Autodock 4.2.6.⁴⁸ In all cases, the same grid size was used, which corresponded to the size resulting from the union of all ligands in a single structure, plus 10 Å in all axes. As for the center of the grid, it corresponded to the center of the union of all the ligands in a single structure. Affinity values underwent normality test (Shapiro-Wilk's test), error variance homogeneity (Bartlett's test), analysis of variance (ANOVA, $P < 0.05$), and separation of means through Scott and Knott test.⁵¹

Mitogen-activated protein kinase

The three-dimensional structures of the mitogen-activated protein kinase 6sot³⁶ and all proteins with similarities of amino acid sequences equal to 100% in relation to the amino acid sequence of 6sot, were obtained from the RCSB Protein Data Bank.⁵² Calculation of Hamming dissimilarity, removal of alternation locations, and three-dimensional alignments were done as described above. Two three-dimensional structures of mitogen-activated protein kinases produced by *Arabidopsis thaliana* (L.) Heynh., with amino acid sequence similarities equal to or higher than 30% in relation to 6sot, were also obtained from the RCSB Protein Data Bank and submitted to the same procedure. Only those proteins (produced by plants or not) that were not mutants and had no missing residue in the binding site or close to it, were selected for the next step.

Using the same procedure described above for rigid alignment, the most stable conformations of compounds **2c** and **2d** underwent superposition to the three-dimensional structures of the compound LOQ (1-phenylpyrrolidine-2,5-dione), which was in the same conformation and position observed in 6sot. Then, the coordinates of **2c**, **2d**, LOQ, and LOK (dimethyl benzene-1,3-diylbiscarbamate), were manually combined with the coordinates of protein atoms in the mitogen-activated protein kinases 1lew,⁵³ 4ka3,⁵⁴ 4loo,⁵⁵ 4lop,⁵⁵ 4loq,⁵⁵ 4tyh,⁵⁶ 5lar,⁵⁷ 5r8u,⁵⁸ 5r8v,⁵⁸ 5r9a,⁵⁸ 5r90,⁵⁸ 5ra0,⁵⁸ 6sfi,⁵⁹ 6so1,⁵⁸ 6so2,⁵⁸ 6so4,⁵⁸ 6sod,⁵⁸ 6soi,⁵⁸ 6sot,⁵⁸ 6sou,⁵⁸ 6y4t,⁶⁰ and 6zwp.⁶⁰ The complexes underwent energy minimization, conversion to the pdbqt format, and calculations of affinity values as described above.

Results and Discussion

Synthesis

Despite the numerous methodologies available for the synthesis of amides, the criteria used to be selected in this work were the reaction time, the ease of purification of the product and the yield.^{15,61-63} The dienamides (**2a-2h**) were prepared by one-pot reaction, where, through treatment with thionyl chloride, sorbic acid (**1**) was converted into its respective acyl chloride. In the sequence, the acyl chloride provided the formation of dienamides by reaction with various anilines (Scheme 1).¹⁸

The formation of dienamides (**2a-2h**) was confirmed by infrared analysis. The band in the region of 3300 cm⁻¹ was assigned to N–H stretching and the band around 1655 cm⁻¹ refers to the stretching of the conjugated amide carbonyl.⁶¹ Furthermore, the appearance of the aromatic system signals,

from the aniline ring, in the ¹H and ¹³C NMR spectra, in addition to the observation of the expected mass values (described in the SI section, “Chemicals” sub-section) confirm the formation of the products.

The regioselective epoxidation of dienamides was achieved by reaction with MCPBA in dichloromethane. Six new compounds were prepared and identified by IR spectroscopy which showed bands around 1240 and 835 cm⁻¹ referring to the symmetric and asymmetric stretching of the C–O–C bond in the epoxide ring. Furthermore, by analyzing the NMR and mass spectra, it was possible to confirm the formation of the monoepoxidized products. The ¹H and ¹³C NMR spectra of the synthesized compounds are shown in the SI section (Figures S11-S38).

Due to the epoxidation mechanism only the *trans* product was formed. The regioselectivity was achieved under the reaction conditions employed. Theoretical studies carried out by our group,²⁰ showed that the epoxide formed (**VIII**) is thermodynamically more stable than the other putative epoxide by 13.37 kJ mol⁻¹ (Figure 1). This energetic barrier arising from the different electrophilicity of the π systems more and less effectively conjugated to the carbonyl ensured the formation of mono-epoxidized products.

Biological activity

Compounds **1**, **2a-2h**, and **3a-3f** were evaluated as growth regulators of monocots and dicots. The phytotoxic capacity of each compound was evaluated against five different species, and the experiment was carried out at four different concentrations and in triplicate with 20 seeds in each analysis. Thus, a total of 60 seeds were used for each concentration for all species. The results of the bioassays were presented using bar graphs (SI section, Figures S1-S10) with the values of stimulus and inhibition of the aerial and root parts of the seeds evaluated according to the positive and negative controls.

Seeds of sorghum, onion, cucumber, and lettuce present a relatively short lifecycle, which allows testing to be performed in a shorter period compared to using whole plant cultures. Seed cultures are easy to handle and can be evaluated based on parameters such as germination, root growth, leaf development, among others. These parameters provide valuable information about the effects of herbicides on plants. The use of seed cultures in herbicide trials allows greater experimental control and greater reproducibility of results. These seeds can be obtained consistently and uniformly, which helps to reduce variations between trials. Beggartick plants are found in various regions worldwide, primarily in humid areas or near bodies of water. From an

agricultural perspective, beggartick can pose a problem as it competes with crops for essential resources like nutrients, water, and sunlight. Hence, beggartick seeds were included in the bioassays to represent a weed species.

The conversion of sorbic acid to amides and the epoxidation of this scaffold produced, in general, compounds with phytotoxic activity superior to the acid precursor.

Allium cepa, a monocotyledonous plant

All compounds tested inhibited shoot growth. Compound **2d** was the most active compound, inhibiting (62%) of growth at a concentration of 250 μM , while the commercial herbicide *S*-metolachlor inhibited (51%) at a concentration of 500 μM . Compounds **2c** and **3b** also exhibited good inhibition, with (46%) and (41%) inhibition at 500 μM , respectively, but were less effective than *S*-metolachlor.

Noteworthy results were obtained with compounds **3b** and **3d**, which caused (67%) inhibition in the root section, and compound **2d**, which exhibited a better outcome than the control by inhibiting (75%) of root growth at 500 μM .

In addition, other compounds also showed excellent results, such as **2c**, **3e**, and **3f**, which showed inhibition of (65%), (62%), and (58%), respectively.

Overall, the modifications performed on the starting material **1** yielded satisfactory effects on phytotoxic activity, resulting in high inhibition of both shoot and root growth, compared to sorbic acid. These findings led us to conclude that amides and epoxides are important classes of compounds for phytotoxic activity in onion seeds. In particular, the epoxidation of **2b** to produce **3b** led to increased phytotoxic activity against shoot growth. With respect to the root section, compounds **3b**, **3e**, and **3f** demonstrated improvements compared to the starting materials **2b**, **2f**, and **2g**.

Furthermore, compound **2d** exhibited superior inhibition compared to the commercial herbicide for both shoot and root growth, indicating the importance of the naphthyl group for the activity of the compound (Figure 2).

Cucumis sativus, a dicotyledonous plant

When evaluating shoot growth, compounds **2b**, **2c**, **2d**, **3e**, and **3f** inhibited growth by 39, 46, 46, 37, and 50%, respectively, at a concentration of 500 μM . These results demonstrate higher phytotoxic activity compared to *S*-metolachlor, which inhibited 35% at the same concentration. Compounds **2a**, **2e**, **3b**, **3c**, and **3d** showed similar results to the commercial herbicide at 500 μM .

Evaluating the shoot results, compounds **2b**, **2c**, **2d**, **2e**, **3b**, **3e**, and **3f** exhibited a similar capacity for

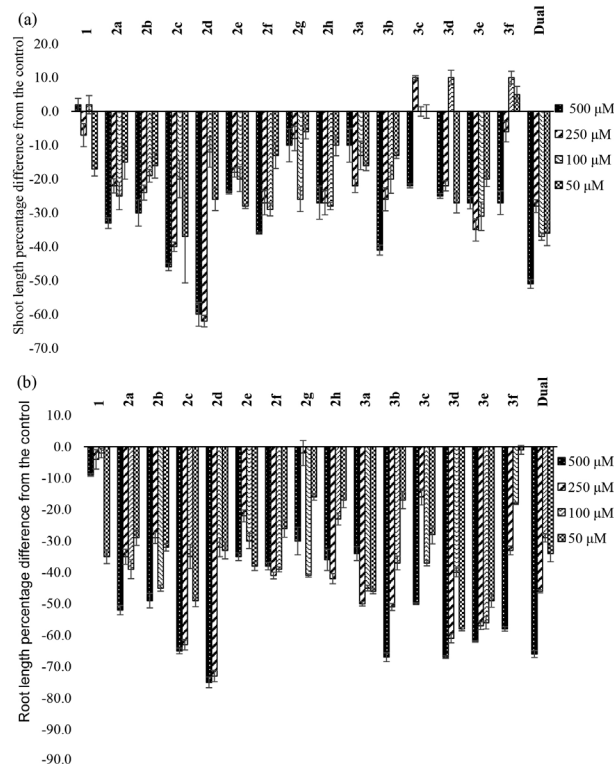


Figure 2. (a) Shoot and (b) root length of *Allium cepa* in relation to the control solution. Values are expressed as the percentage difference from the control. The error bars represent the standard deviation.

inhibiting seed growth as the positive control. Notably, the epoxidation products **3e** and **3f** exhibited better phytotoxic activity on the shoots than the dienamide precursor (SI section, Figures S3, and S4).

Lactuca sativa, dicotyledonous plant

The better values of inhibition of *L. sativa* were from the aerial parts of the plant, for compounds **2c** (44%) and **2d** (44%) at 500 μM .

For shoot inhibition, **3e** and **3f** showed better inhibition (around 40% at 500 μM). Interestingly, except for **2a**, the epoxidation of dienamides does not increase the phytotoxicity of the amides in the shoot. However, in the root part, the epoxidation of **2f** and **2g** increased the activity by 800 and 100%, respectively, at 500 μM (SI section, Figures S9 and S10).

Bidens pilosa, a dicotyledonous plant

Regarding the shoot, all evaluated substances inhibited growth, in special, **2a**, **2c**, **2d**, **3a**, **3b**, **3c**, **3e**, and **3f**, but with less effect than the commercial herbicide *S*-metolachlor (60%, 500 μM).

Analyzing the effect of the substances in the root part (500 μM) we observed that compounds **2e** (62%), **3b** (77%), **3c** (72%), and **3e** (66%) presented a superior inhibitory effect than *S*-metolachlor (60%). Additionally, compounds

3a and **3f** exhibited good inhibitory values of (55%) and (57%), respectively, although less than the positive control (SI section, Figures S5 and S6).

Sorghum bicolor, a monocotyledonous plant

In general, the synthesized substances were not active in inhibiting the development of *S. bicolor* (SI section, Figures S1 and S2). This experimental observation draws attention to the fact that *S. bicolor* is a crop normally sensitive to herbicides. For the application of *S*-metolachlor in sorghum crops, it is recommended to use seed protective agents such as fluxofenim to guarantee selectivity in population control of pests and protect the harvest from the non-selective action of the herbicide.⁶²

In this regard, our attention was drawn to the high selectivity of some molecules against species other than *S. bicolor*. Specifically, compounds **2d**, **3b**, **3e**, and **3f** showed low phytotoxicity to *S. bicolor* while they were able to inhibit, more efficiently than *S*-metolachlor, the root and aerial growth of the other evaluated species. The selectivity value for the selected compounds was calculated using equation 1 and is shown in Figure 3.

$$\text{Selectivity} = \frac{\text{percentage inhibition of target species}}{\text{percentage inhibition of } S. bicolor} \quad (1)$$

High values of phytotoxic selectivity acting on the root part of the plants were found for compound **3f** (*B. pilosa* (57%), *A. cepa* (58%), *C. sativus* (56%), and *L. sativa* (39%)).

These results are interesting because they point to a new chemical scaffold that can be exploited to develop new herbicides for use in sorghum crops with less impact on the plantation due to the high selectivity to inhibit the development of other species.

Computational study

The pharmacophoric search resulted in the initial selection of 14 proteins (1c84, 1vea, 2dsa 3kqv, 3tzs, 4f1q, 4g27, 4hvd, 5c9w, 5x20, 6ekw, 6sot, 1o7g, and 3vlm). However, according to the search made in plant genomes with the amino acid sequences of these proteins, only protein tyrosine phosphatase 1c84⁶³ and mitogen-activated protein kinase 6sot⁵⁸ seem important to explain the experimental results, as these are the only proteins for which similar sequences were found in plants (SI section, Tables S1 and S2). Especially, proteins in *Allium* spp. (SI section, Table S3), *Cucumis* spp. (SI section, Tables S4 and S5), *Lactuca* spp. (SI section, Tables S6 and S7), and *Sorghum* spp. (SI section, Tables S8 and S9).

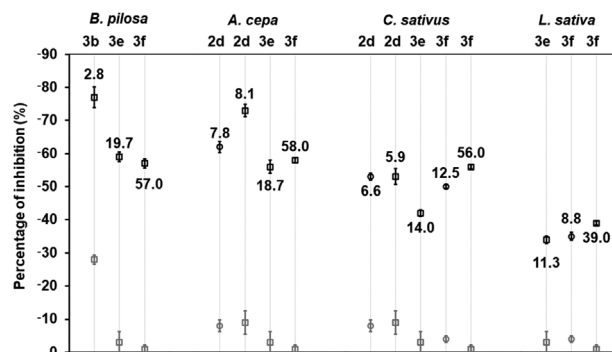


Figure 3. Inhibition percentage and selectivity of compounds **2d** (250 μ M), **3b** (500 μ M), **3e** (100 μ M), and **3f** (500 μ M) of *S. bicolor* (grey) and other species (black). Symbol (□) indicates inhibition of the root, and (○) indicates inhibition of shoot. The number next to the symbols (□) and (○) represents the selectivity of the compound with respect to inhibition of *S. bicolor* at the same concentration (equation 1). Bars entered in the symbols (□) and (○) represent the standard deviation. All compounds were statistically different from *S*-metolachlor (ANOVA, $p < 0.05$).

The results obtained so far suggest that the substances **2c** and **2d** may form complexes with the protein tyrosine phosphatase 1c84 and mitogen-activated protein kinase 6sot, whose amino acid sequences are very similar to the various enzymes produced by plants. Therefore, it is likely that compounds **2c** and **2d** may also inhibit these enzymes.

Protein tyrosine phosphatases remove phosphate groups from phosphorylated tyrosine residues on proteins. They are involved in abscisic acid,⁶⁴ cytokinins,⁶⁵ and brassinosteroid-dependent processes⁶⁵ in plants. Furthermore, these enzymes are also involved in the regulation of stomatal movement⁶⁶ and response to phytopathogens.⁶⁶ Therefore, they are of great importance to plants. In the specific case of protein tyrosine phosphatase 1c84, there are 298 amino acid residues. Its binding site is occupied by compound OLN, which is an inhibitor of these enzymes and has overlap with compounds **2c** and **2d** (SI section, Figure S39).

No three-dimensional structure was found for protein tyrosine phosphatases produced by *Allium cepa* L., *Bidens pilosa* L., *Cucumis sativus* L., *Lactuca sativa* L., or *Sorghum bicolor* L. Therefore, the work was continued with the structure of 1c84, which, as already mentioned, has a sequence of amino acids very similar to those produced by several plants of the same genera of the mentioned plant species (SI section, Tables S1-S9). Furthermore, 5 proteins (1c83, 1c85, 1c87, 1c88, and 1ecv) of type tyrosine phosphatases, were also used, as their amino acid sequences are, at least, 95% equal to the 1c84 sequence. In addition, the root-mean-square deviation (RMSD) values of these enzymes concerning 1c84 are all below 0.3 Å (SI section, Table S10).

When the three-dimensional structures of enzymes A and B are aligned, their inhibitors are perfectly overlapped (SI section, Figure S40). Consequently, the methodology

adopted in the present work consisted of aligning the most stable conformations of substances **2c** and **2d** to these inhibitors, to form complexes of these substances with proteins. Once the energies of the complexes formed were minimized, the affinities of the ligands for the active sites of the proteins were calculated, which allowed us to observe that compounds **2c** and **2d** tend to have less affinities for such sites than the other compounds (SI section, Figure S41).

These results suggest that **2c** and **2d** are not good protein tyrosine phosphatase inhibitors, which is an indication that the way these substances act against plants is not related to the inhibition of these enzymes.

Mitogen-activated protein kinases (MAPKs) are enzymes that phosphorylate the amino acid residues serine and threonine, in various proteins. In the specific case of plants, it is observed, for example, that such enzymes are related to plants' resistance to pathogens,⁶⁵ stress, and hormonal responses.⁶⁷ Therefore, these enzymes are very important for plants. In the case of the enzyme 6sot, there are 381 amino acid residues and four binding sites. One of them, called the noncanonical site, is used by the enzyme to form a complex with TAB1,⁵⁸ which activates MAPKs.^{52,55,68} Therefore, any substance that binds efficiently to the non-canonical site can prevent MAPK activation and, consequently, can interfere with the activity of these enzymes. One such substance is LOQ (1-phenylpyrrolidine-2,5-dione), which is in the noncanonical site of the MAPK 6sot and was selected during the search for pharmacophorically similar substances to **2c** and **2d** (Figure 4).

No three-dimensional structure was found for MAPKs produced by *Allium cepa* L., *Bidens pilosa* L., *Cucumis sativus* L., *Lactuca sativa* L., or

Sorghum bicolor (L.) Moench. Therefore, the work was continued with the structure of 6sot, which, as already mentioned, has a sequence of amino acids very similar to those produced by several plants of the same genera of the mentioned plant species (SI section, Tables S1-S9, and S11).

As there was no other ligand with a structure like LOQ, anchored in the noncanonical site of a mitogen-activated protein kinase, it was decided to align the more stable conformations of **2c** and **2d** to LOQ, for the formation of the various complexes that, once optimized through minimization of their energies, could be subjected to the calculations of ligand affinities for enzymes. It was observed, with both computer programs used, that the substance **2d** has more affinity for the enzymes than the compounds LOQ and LOK, which inhibit the enzyme through binding to the noncanonical site. Regarding compound **2c**, although less efficient than **2d**, its affinity is statistically equal to that calculated for LOQ by both programs. Furthermore, **2c** binds more efficiently to the enzymes than the compounds LOK (SI section, Figure S42). Therefore, these results suggest that compounds **2c** and **2d** can inhibit mitogen-activated protein kinases with amino acid sequences very similar to those produced by plants that were affected by these compounds in the assays carried out in the present work. Consequently, substances **2c** and **2d** are likely to act against these plants through complexation to the noncanonical site of mitogen-activated protein kinases produced by those plants.

Compound **2d** interacts with the amino acid residues ASP124, LEU217, THR218, VAL273, PHE274, ILE275, ALA277 and ASN278, of the enzyme 6sot (Figure 5). Two more than compound LOQ, to which **2d** is superimposed. Probably, this greater number of interactions is one of the factors that contribute to the greater efficiency in the

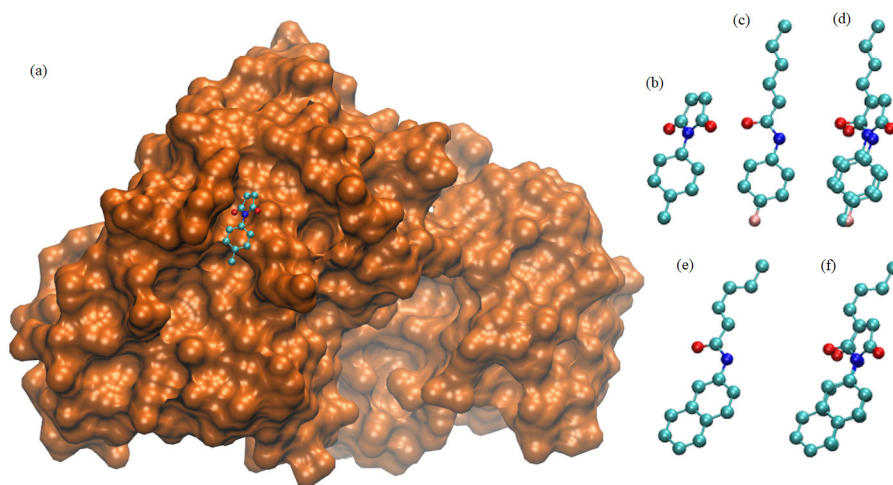


Figure 4. (a) MSMS²⁹ representation of the mitogen-activated protein kinase 6sot (orange), containing the compound LOQ (1-(*p*-tolyl)pyrrolidine-2,5-dione) in its noncanonical binding site. (b) Compound LOQ enlarged and with the same conformation of A; (c) compound **2c**; (d) compound **2c** superimposed on compound LOQ; (e) compound **2d**. (f) compound **2d** superimposed on compound LOQ.

complexation of compound **2d** to the non-canonical site of the enzyme.

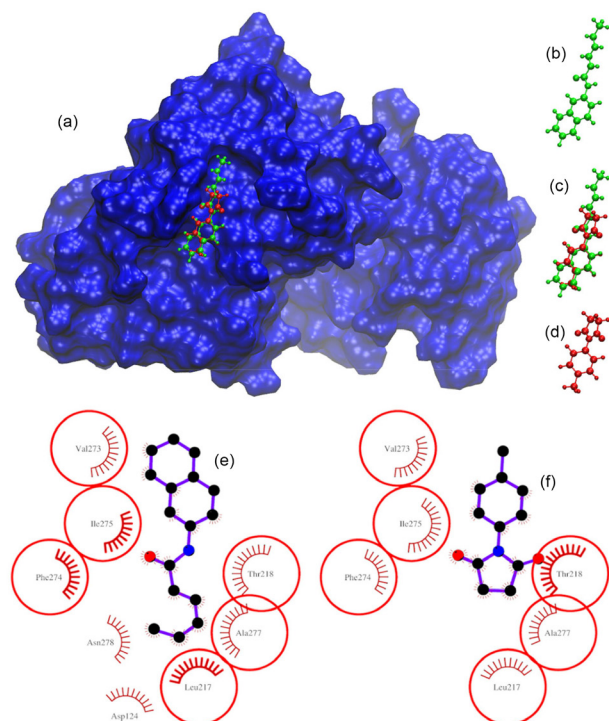


Figure 5. Representations of the interactions of compounds **2d** and LOQ with the mitogen-activated protein kinase 6sot: (a) MSMS³¹ representation of the three-dimensional structure of 6sot containing compounds **2d** (green) and LOQ (red) in the noncanonical site; (b) compound **2d** enlarged and with the same conformation of A; (c) compounds **2d** and LOQ enlarged and with the same conformation of A; (d) compound LOQ enlarged and with the same conformation of A; (e) two-dimensional representation of the interactions of compound **2d** with the enzyme 6sot; (f) two-dimensional representation of the interactions of compound LOQ with the enzyme 6sot. Ligplot+ 2.2.4⁶⁹ and VMD 1.9.3³⁸ were used to prepare the two- and three-dimensional representations, respectively.

Although the compound LOK interacts with the same amino acid residues of the enzyme 6sot with which the compound LOQ interacts, some interactions are not as favorable. This is the case, for example, of the interaction of the carbonyl of the compound LOK with the nonpolar groups of the amino acid residue VAL273. This probably makes the complexing efficiency of the compound LOK to be lower than observed for the other compounds. This problem is not observed with compound **2c**, which interacts with one less amino acid residue than compound **2d** (Figure 6).

Conclusions

In conclusion, all synthesized compounds exhibited activity in seed germination. However, compounds **2c**, **2d**, **3b**, **3e**, and **3f** showed superior activity to the commercial herbicide *S*-metolachlor.

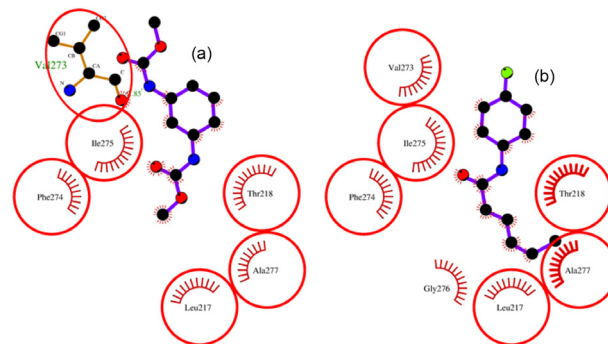


Figure 6. (a) Two-dimensional representation of the interactions of compound LOK with the enzyme 6sot; (b) two-dimensional representation of the interactions of compound **2c** with the enzyme 6sot.

The obtained results suggest that substances **2c** and **2d** could potentially interact with the protein tyrosine phosphatase 1c84 and mitogen-activated protein kinase 6sot, whose amino acid sequences bear a close resemblance to the enzymes produced by plants. This implies that the formation of complexes between the substances and the enzymes is possible.

Furthermore, considering the structural similarities between the enzymes and the targeted proteins, it is likely that substances **2c** and **2d** could inhibit the enzymes as well. Therefore, it is plausible to conclude that the compounds' inhibitory effect on the enzymes may extend to other related enzymes, which could prove useful for potential therapeutic applications. However, further studies are necessary to confirm these findings and explore the compounds' inhibitory mechanism on the enzymes.

Therefore, if these compounds can be produced at a large scale with consistent quality and purity, they could potentially serve as a sustainable and cost-effective alternative to conventional herbicides in agriculture and other industries. However, extensive testing and regulatory approval are necessary before the widespread use of these compounds as herbicides.

Supplementary Information

Supplementary information is available free of charge at <http://jbcs.sbq.org.br> as PDF file.

Acknowledgments

We would like to thank the Brazilian Agencies CNPq, CAPES, RQ-MG, and FAPEMIG for financial support.

Author Contributions

Danielle S. Ramos was responsible for data curation, formal

analysis, investigation, methodology, writing original draft; Elson S. Alvarenga for conceptualization, data curation, funding acquisition, investigation, supervision, writing-original draft, review and editing; Júnio G. Silva for bioassay methodology, writing draft and editing; Cristiane I. Cerceau for bioassay methodology, writing review and editing; Suélen K. Sartori for writing draft and editing; Vania M. T. Carneiro for reviewing the final version; Denilson F. Oliveira for theoretical calculations and formal analysis.

References

- Fujiwara, T.; O'Hagan, D.; *J. Fluorine Chem.* **2014**, *167*, 16. [Crossref]
- Organization for Economic Co-operation and Development (OECD) and Food and Agriculture Organization of the United Nations (FAO); *Agricultural Outlook 2019*, https://www.oecd-ilibrary.org/agriculture-and-food/oecd-fao-agricultural-outlook-2019-2028_agr_outlook-2019-en, accessed in June 2023.
- Tester, M.; Langridge, P.; *Science* **2010**, *327*, 818. [Crossref]
- Zhang, P.; Guan, A.; Xia, X.; Sun, X.; Wei, S.; Yang, J.; Wang, J.; Li, Z.; Lan, J.; Liu, C.; *J. Agric. Food Chem.* **2019**, *67*, 11893. [Crossref]
- Busi, R.; Powles, S. B.; *Pest Manage. Sci.* **2016**, *72*, 1664. [Crossref]
- Chen, L.; Li, J.; Zhu, Y.; Zhao, T.; Guo, L.; Kang, L.; Yu, J.; Du, H.; Liu, D.; *J. Agric. Food Chem.* **2022**, *70*, 1494. [Crossref]
- Zhang, Z. P.; *Weed Biol. Manage.* **2003**, *3*, 197. [Crossref]
- Rodenburg, J.; Johnson, J.-M.; Dieng, I.; Senthilkumar, K.; Vandamme, E.; Akakpo, C.; Allarangaye, M. D.; Baggie, I.; Bakare, S. O.; Bam, R. K.; Bassoro, I.; Abera, B. B.; Cisse, M.; Dogbe, W.; Gbakatchétché, H.; Jaiteh, F.; Kajiru, G. J.; Kalisa, A.; Kamissoko, N.; Sékou, K.; Kokou, A.; Mapiemfu-Lamare, D.; Lunze, F. M.; Mghase, J.; Maïga, I. M.; Nanfumba, D. Niang, A.; Rabeson, R.; Segda, Z.; Sillo, F. S.; Tanaka, A.; Saito, K.; *Food Sec.* **2019**, *11*, 69. [Crossref]
- Alcántara-de la Cruz, R.; de Oliveira, G. M.; de Carvalho, L. B.; da Silva, M. F. G. F.; *Herbicide Resistance in Brazil: Status, Impacts, and Future Challenges*, 19th ed.; IntechOpen: London, UK, 2020.
- O'Sullivan, C. A.; Bonnett, G. D.; McIntyre, C. L.; Hochman, Z.; Wasson, A. P.; *Agric. Syst.* **2019**, *174*, 133. [Crossref]
- Li, X.-x.; Liu, Y.; He, L.-f.; Gao, Y.-y.; Mu, W.; Zhang, P.; Li, B.-x.; Liu, F.; *J. Agric. Food Chem.* **2020**, *68*, 1198. [Crossref]
- Asaduzzaman, M.; Pratley, J. E.; Luckett, D.; Lemerle, D.; Wu, H.; *Arch. Agron. Soil Sci.* **2020**, *66*, 427. [Crossref]
- Renton, M.; Busi, R.; Neve, P.; Thornby, D.; Vila-Aiub, M.; *Pest Manage. Sci.* **2014**, *70*, 1394. [Crossref]
- Fennimore, S. A.; Cutulle, M.; *Pest Manage. Sci.* **2019**, *75*, 1767. [Crossref]
- Mathieson, J. E.; Crawford, J. J.; Schmidtman, M.; Marquez, R.; *Org. Biomol. Chem.* **2009**, *7*, 2170. [Crossref]
- Chowdhury, M.; Mandal, S. Banerjee, S.; Zajc, B.; *Molecules* **2014**, *19*, 4418. [Crossref]
- Aguiar, A. R.; Alvarenga, E. S.; Lopes, M. C.; dos Santos, I. B.; Galdino, T. V.; Picanço, M. C.; *J. Environ. Sci. Health, Part B* **2016**, *51*, 579. [Crossref]
- Lopes, M. C.; Alvarenga, E. S.; Aguiar, A. R.; Santos, I. B.; Silva, G. A.; Arcanjo, L. P.; Picanço, M. C.; *Quim. Nova* **2018**, *41*, 375. [Crossref]
- Sartori, S. K.; Alvarenga, E. S.; Franco, C. A.; Ramos, D. S.; Oliveira, D. F.; *Pest Manage. Sci.* **2018**, *74*, 1637. [Crossref]
- Aguiar, A. R.; Alvarenga, E. S.; Oliveira, R. P.; Carneiro, V. M. T.; Moura, G. L.; *J. Mol. Struct.* **2018**, *1165*, 312. [Crossref]
- de Alvarenga, E. S.; Saliba, W. A.; Milagres, B. G.; *Quim. Nova* **2005**, *28*, 927. [Crossref]
- Cvetovich, R. J.; DiMichele, L.; *Org. Process Res. Dev.* **2006**, *10*, 944. [Crossref]
- Adegas, F. S.; Voll, E.; Prete, C. E. C.; *Planta Daninha* **2003**, *21*, 21. [Crossref]
- ImageJ*; Wayne Rasband, Bethesda, Maryland, USA. [Link] accessed in June 2023
- ChemSketch*; Advanced Chemistry Development, Inc., Toronto, Ontario, Canada, 2012.
- O'Boyle, N. M.; Banck, M.; James, C. A.; Morley, C.; Vandermeersch, T.; Hutchison, G. R.; *J. Cheminf.* **2011**, *3*, 1758. [Crossref]
- Tosco, O. P.; Balle, T.; Shiri, F.; *J. Comput.-Aided Mol. Des.* **2011**, *25*, 777. [Crossref]
- Stewart, J. J. P.; *MOPAC (Molecular Orbital PACKage)*; <http://openmopac.net>, accessed in June 2023.
- Lešnik, S.; Štular, T.; Brus, B.; Knez, D.; Gobec, S.; Janežič, D.; Konc, J.; *J. Chem. Inf. Model.* **2015**, *55*, 1521. [Crossref]
- Feng, Z.; Chen, L.; Maddula, H.; Akcan, O.; Oughtred, R.; Berman, H. M.; Westbrook, J.; *Bioinformatics* **2004**, *20*, 2153. [Crossref]
- Sanner, M. F.; Olson, A. J.; Spohner, J.-C.; *Biopolymers* **1996**, *38*, 305. [Crossref]
- National Center for Biotechnology Information (NCBI); <https://www.ncbi.nlm.nih.gov/>, accessed in June 2023.
- Altschul, S. F.; Madden, T. L.; Schäffer, A. A.; Zhang, J.; Zhang, Z.; Miller, W.; Lipman, D. J.; *Nucleic Acids Res.* **1997**, *25*, 3389. [Crossref]
- Boratyn, G. M.; Schäffer, A. A.; Agarwala, R.; Altschul, S. F.; Lipman, D. J.; Madden, T. L.; *Biol. Direct* **2012**, *7*, 12. [Crossref]
- Berman, H. M.; Westbrook, J.; Feng, Z.; Gilliland, G.; Bhat, T. N.; Weissig, H.; Shindyalov, I. N.; Bourne, P. E.; *Nucleic Acids Res.* **2000**, *28*, 235. [Crossref]
- Okonechnikov, K.; Golosova, O.; Fursov, M.; *Bioinformatics* **2012**, *28*, 1166. [Crossref]
- Sievers, F.; Higgins, D. G.; *Protein Sci.* **2018**, *27*, 135. [Crossref]

38. Martínez, L.; Andreani, R.; Martínez, J. M.; *BMC Bioinf.* **2007**, *8*, 306. [Crossref]
39. Humphrey, W.; Dalke, A.; Schulten, K.; *J. Mol. Graphics* **1996**, *14*, 33. [Crossref]
40. Hu, J.; Liu, Z.; Yu, D.-J.; Zhang, Y.; *Bioinformatics* **2018**, *34*, 2209. [Crossref]
41. ChemAxon, <https://chemaxon.com/>, accessed in June 2023.
42. Andersen, H. S.; Iversen, L. F.; Jeppesen, C. B.; Branner, S.; Norris, K.; Rasmussen, H. B.; Møller, K. B.; Møller, N. P.; *J. Biol. Chem.* **2000**, *275*, 7101. [Crossref]
43. Iversen, L. F.; Andersen, H. S.; Branner, S.; Mortensen, S. B.; Peters, K.; Norris, G. H.; Olsen, C. B.; Jeppesen, O. H.; Lundt, B. F.; Ripka, W.; Møller, K. B.; *J. Biol. Chem.* **2000**, *275*, 10300. [Crossref]
44. Pettersen, E. F.; Goddard, T. D.; Huang, C. C.; Couch, G. S.; Greenblatt, D. M.; Meng, E. C.; Ferrin, T. E.; *J. Comput. Chem.* **2004**, *25*, 1605. [Crossref]
45. Maier, J. A.; Martinez, C.; Kasavajhala, K.; Wickstrom L.; Hauser, K. E.; Simmerling, C.; *J. Chem. Theory Comput.* **2015**, *11*, 3696. [Crossref]
46. Jakalian, A.; Jack, D. B.; Bayly, C. I.; *J. Comput. Chem.* **2002**, *23*, 1623. [Crossref]
47. Wang, J.; Wang, W.; Kollman, P. A.; Case, D. A.; *J. Mol. Graph. Modell.* **2006**, *25*, 247. [Crossref]
48. Morris, G. M.; Huey, R.; Lindstrom, W.; Sanner, M. F.; Belew, R. K.; Goodsell, D. S.; Olson, A. J.; *J. Comput. Chem.* **2009**, *30*, 2785. [Crossref]
49. Alhossary, A.; Handoko, S. D.; Mu, Y.; Kwoh, C. K.; *Bioinformatics* **2015**, *31*, 2214. [Crossref]
50. Trott, O.; Olson, A. J.; *J. Comput. Chem.* **2010**, *31*, 455. [Crossref]
51. Scott, A. J.; Knott, M.; *Biometrics* **1974**, *30*, 507. [Crossref]
52. Bigeard, J.; Hirt, H.; *Front Plant Sci.* **2018**, *9*, 469. [Crossref]
53. Chang, C. I.; Xu, B.-e.; Akella, R.; Cobb, M. H.; Goldsmith, E. J.; *Mol Cell.* **2002**, *9*, 1241. [Crossref]
54. Xin, F. J.; Wu, J.W.; *Sci. China: Life Sci.* **2013**, *56*, 653. [Crossref]
55. De Nicola, G. F.; Martin, E. D.; Chaikuad, A.; Bassi, R.; Clark, J.; Martino, L.; Verma, S.; Sicard, P.; Tata, R.; Atkinson, R. A.; Knapp, S.; Conte, M. R.; Marber, M. S.; *Nat. Struct. Mol. Biol.* **2013**, *20*, 1182. [Crossref]
56. Protein Data Bank, <https://www.rcsb.org/structure/4TYH>, accessed in June 2023.
57. Petersen, L. K.; Blakskjær, P.; Chaikuad, A.; Christensen, A. B.; Dietvorst, J.; Holmkvist, J.; Knapp, S.; Kořínek, M.; Larsen, L. K.; Pedersen, A. E.; Röhm, S.; Sløk, F. A.; Hansen, N. J. V.; *MedChemComm* **2016**, *7*, 1332. [Crossref]
58. Nichols, C.; Ng, J.; Keshu, A.; Kelly, G.; Conte, M. R.; Marber, M. S.; Fraternali, F.; De Nicola, G. F.; *J. Med. Chem.* **2020**, *63*, 7559. [Crossref]
59. Röhm, S.; Berger, B.-T.; Schröder, M.; Chaikuad, A.; Winkel, R.; Hekking, K. F. W.; Benningshof, J. J. C.; Müller, G.; Tesch, R.; Kudolo, M.; Forster, M.; Laufer, S.; Knapp, S.; *J. Med. Chem.* **2019**, *62*, 10757. [Crossref]
60. Röhm, S.; Schröder, M.; Dwyer, J. E.; Widdowson, C. S.; Chaikuad, A.; Berger, B.-T.; Joerger, A. C.; Krämer, A.; Harbig, J.; Dauch, D.; Kudolo, M.; Laufer, S.; Bagley, M. C.; Knapp, S.; *Eur. J. Med. Chem.* **2020**, *208*, 112721. [Crossref]
61. Gao, X.; Tang, J.; Liu, H.; Liu, L.; Kang, L.; Chen, W.; *J. Enzyme Inhib. Med. Chem.* **2018**, *33*, 519. [Crossref]
62. Shi, L.; Yang, J.; Wen, X.; Huang, Y.-Z.; *Tetrahedron Lett.* **1988**, *29*, 3949. [Crossref]
63. Hu, Y.; Floss, H. G.; *J. Am. Chem. Soc.* **2004**, *126*, 3837. [Crossref]
64. Ghelis, T.; Bolbach, G.; Clodic, G.; Habricot, Y.; Miginiac, E.; Sotta, B.; Jeannette, E.; *Plant Physiol.* **2008**, *148*, 1668. [Crossref]
65. Shankar, A.; Agrawal, N.; Sharma, M.; Pandey, A.; Pandey, G. K.; *Curr. Genomics* **2015**, *16*, 224. [Crossref]
66. MacRobbie, E. A. C.; *Proc. Natl. Acad. Sci. U. S. A.* **2002**, *99*, 11963. [Crossref]
67. Cristina, M.; Petersen, M.; Mundy, J.; *Annu. Rev. Plant Biol.* **2010**, *61*, 621. [Crossref]
68. Thapa, D.; Nichols, C.; Bassi, R.; Martin, E. D.; Verma, S.; Conte, M. R.; De Santis, V.; De Nicola, G. F.; Marber, M. S.; *Mol Cell Biol.* **2018**, *38*, e00409-17. [Link] accessed in June 2023
69. Laskowski, R. A.; Swindells, M. B.; *J. Chem. Inf. Model.* **2011**, *51*, 2778. [Crossref]

Submitted: April 20, 2023

Published online: July 11, 2023